MSUCL-203
January 1976

A Coupled-Channel Born Approximation Analysis of $^{22}Ne(p,t)^{20}Ne$ and $^{24}Mg(p,t)^{22}Mg$ using Shell-Model Wavefunctions*

C.H. King, M.A.M. Shahabuddin and B.H. Wildenthal

Cyclotron Laboratory, Michigan State University
East Lansing, Michigan 48824

ABSTRACT

Coupled-channel Born approximation calculations for the reactions $^{22}Ne(p,t)^{20}Ne$ and $^{24}Mg(p,t)^{22}Mg$ to the 0^+, 2^+, and 4^+ members of the ground-state rotational bands have been carried out. The two-nucleon transfer spectroscopic amplitudes were determined from shell-model wavefunctions, the calculation of inelastic excitations was based on the collective model, and the reaction space was limited to the first 0^+, 2^+, and 4^+ states in each nucleus. The measured cross sections in the case of $^{22}Ne(p,t)$ are reasonably well described by this model. However, significant deviations were observed between the calculated cross sections and the experimental data for the $^{24}Mg(p,t)$ transitions to the 2^+ and 4^+ states. These discrepancies are possibly attributable to multistep processes involving higher-lying states in ^{24}Mg not included in the reaction space. The effects on the calculations of other possible inadequacies of the reaction model and uncertainties in the parameters of this model are discussed.

[NUCLEAR REACTIONS: $^{22}Ne(p,t)$, E=39.8 MeV. $^{24}Mg(p,t)$, E=42.0 MeV; calculated $\sigma(\theta)$ using coupled-channel Born approximation and shell-model spectroscopic amplitudes.]

*Work supported by the National Science Foundation.

1. INTRODUCTION

Considerable effort has been devoted in recent years toward achieving improved wave functions in a shell-model basis for the states of nuclei in the A=16-40 region. Transfer-reaction experiments are a potentially useful tool for testing the quality of such wavefunctions, since the measured cross sections should be directly related to the overlaps between the wavefunctions of the initial and final states as long as only direct, one-step reaction processes are significant. Unfortunately, it is questionable whether a one-step reaction model is applicable to transfer reactions on the highly collective nuclei in the middle of this region. In fact, increasing evidence seems to indicate that multistep processes involving inelastic excitations of the collective states are an essential component of such reactions.

When multistep effects are important, it is necessary to replace the usual analysis based on the distorted-wave Born approximation (DWBA) with one using the coupled-channel Born approximation (CCBA). This necessarily complicates the relation between the theoretical wavefunction and the experimental cross sections, since any one cross section will depend coherently on matrix elements connecting several states in the initial and final nuclei while the DWBA requires only one. In particular, matrix elements between the wavefunctions of all states coupled strongly by inelastic scattering to the initial and final states must be included. Nevertheless, since shell-model wavefunctions can be used to calculate such matrix elements, a test of these wavefunctions would seem to be possible within the framework of the CCBA. In this paper we present an attempt at such an analysis.

One difficulty with this approach becomes evident very quickly. A completely consistent test of shell-model wavefunctions by calculating transfer-reaction cross sections by the CCBA method would use shell-model matrix elements to determine the spectroscopic amplitudes not only for the transfer transitions connecting states of the initial and final nuclei but also for the inelastic transitions coupling the various states within each nucleus. However, shell-model wavefunctions based on a limited set of active orbitals are known to underpredict the strength of inelastic coupling because of core-polarization effects. This is particularly true for collective states, which are the very ones which must be considered in a CCBA analysis. Since one would like to isolate this well known problem from any difficulties the wavefunctions may have in predicting transfer transitions, it is advisable to determine the inelastic matrix elements by some empirical method. This could be done, for example, by renormalizing shell-model inelastic matrix elements by using measured electromagnetic transition rates.[1] In this work, however, we have adopted instead a more phenomenological approach, using inelastic matrix elements based on the collective model with deformation parameters determined by fits to inelastic scattering data.

The examples we have chosen to examine are the reactions $^{22}Ne(p,t)^{20}Ne$ and $^{24}Mg(p,t)^{22}Mg$. The cross sections considered are those to the first 0^+, 2^+, and 4^+ states of the residual nucleus, which we treat as forming a ground-state rotational band ($K^\pi=0^+$). This restriction to (p,t) transitions between 0^+ bands keeps the number of states which must be considered

in the calculations and their spins relatively small. Thus, the coupled-channel calculations are kept to a manageable size. In addition, the two-nucleon transfer reactions like (p,t) are interesting in their own right since unlike single-nucleon transfer reactions, they are sensitive to the relative phases of various components of the shell-model wavefunctions. Of course, this sensitivity is an indirect one and becomes potentially more obscure when several transitions must be considered simultaneously as in the CCBA.

2. ANALYSIS PROCEDURE

In the coupled-channel Born approximation, which has been described extensively elsewhere,[2,3] the transfer interaction is treated to first order as in the DWBA but the inelastic coupling is taken to all orders, with the one-channel distorted waves of the DWBA replaced by generalized distorted waves which are solutions of coupled equations describing the interaction between the projectile and nucleus in the entrance and exit channels. The calculations presented here were performed with the computer code LISA written by R.J. Ascuitto,[4] which uses the source-term method[3] for evaluating the CCBA transition amplitude.

The two-neutron transfer form factors were determined from spectroscopic amplitudes based on the shell-model wavefunctions of Chung and Wildenthal,[5] which were obtained using a full 1s-0d shell basis. The single-particle bound-state wave functions were generated in a Woods-Saxon potential well with a radius of $1.25\ A^{1/3}$ fm (where A is the mass number of the final nucleus) and a diffuseness of 0.65 fm. The spin-orbit coupling was chosen to be 30 times the Thomas value, and the well-depth was adjusted

so as to bind the single-particle state at one-half the two-nucleon separation energy for each transfer route. The form factors were evaluated using the computer program DWUCK,[6] which used the Bayman-Kallio[7] procedure.

The inelastic matrix elements were based on the collective model, assuming that the nuclear states involved are members of a $K^{\pi}=0^{+}$ rotational band. Expressions for the matrix elements in this model are given, for example, in reference 8. In this approximation the matrix elements are completely determined by the parameterization of the nuclear surface. We have assumed that the surface can be described in terms of a spherical harmonic expansion limited to quadrupole (β_2) and hexadecapole (β_4) terms, with the two deformation parameters determined empirically by fitting inelastic scattering cross sections in a coupled-channel calculation. The various optical-model and deformation parameters employed in our calcuations are listed in Tables 1, 2 and 4. Details of their determination are described below.

Unless otherwise specified all calculations presented here have been performed using a coupling space involving the 0^{+}, 2^{+}, and 4^{+} states of the ground-state rotational band in both initial and final nuclei. All allowed inelastic and transfer transitions within this space have been included. The effects of spin-orbit coupling and Coulomb excitation were found to be small and thus were ignored.

One problem with this hybrid shell-model/collective-model analysis procedure is to assure that the phases of the wavefunctions of the same states within the two models are consistent. In the present work this was accomplished by calculating inelastic

form factors from the shell-model wavefunctions. The quadrupole form factors were found to be qualitatively similar to the real part of the quadrupole form factors generated within the collective model. Thus a comparison of the signs of these two sets of inelastic form factors established the relative phases of the wavefunctions in the two models. The signs of the spectroscopic amplitudes listed in Tables 3 and 5 reflect the adjustment of the phases of the shell-model wavefunctions by this technique to be consistent with the phases of the usual collective-model wavefunctions.

3. RESULTS: $^{22}Ne(p,t)^{20}Ne$

The nuclides ^{22}Ne and ^{20}Ne are known to possess strongly deformed, relatively pure ground-state rotational bands. The $^{22}Ne(p,t)$ reaction to the ^{20}Ne ground band is thus an excellent test case for CCBA calculations in this mass range. Such calculations have already been attempted by Olsen et al.[9] who also measured differential cross sections for this reaction at 39.8 MeV. These authors adopted a collective-model approach to describe both the inelastic and transfer matrix elements. Two models were tried for the intrinsic states of ^{22}Ne and ^{20}Ne and hence for the transfer amplitudes: a pure Nilsson model and a pairing-mixed Nilsson model. With the latter model, CCBA angular distributions were obtained which were in reasonably good agreement in relative magnitude and shape with the measured cross sections.

We have performed CCBA calculations for the same reactions using the mixed shell- and collective-model approach described in Section 2. The results are shown in Figure 1 compared with the data of Olsen et al. Here we have used the same optical-model

and deformation parameters as those of reference 9. These parameter sets are listed as #1 in Tables 1 and 2, and the two-nucleon transfer spectroscopic amplitudes are listed in Table 3. These calculations differ from those of Olsen et al. not only in the use of shell-model wavefunctions to determine the transfer amplitudes but also in the use of 0^+- 2^+- 4^+ inelastic coupling in both initial and final nuclei. The calculations of Olsen et al. included only a 0^+-2^+ coupling in the entrance channel; however, we found the addition of the coupling to the 4^+ state to make only a small change in the final calculated cross sections. DWBA calculations using the same form factors and optical-model parameters are shown for comparison. It is evident that the CCBA calculations give a good reproduction of the experimental relative strengths of the three transitions and a reasonable approximation of the general features of the angular distributions. A comparison with the DWBA shows that the effects of the multistep processes occur mainly in the shapes of the 2^+ and 4^+ transitions and the strength of the 4^+ transition.

The two-nucleon transfer strength constant D_0^2, where we use the same definition as given in Baer et al.,[10] was chosen separately for the DWBA and CCBA calculations shown in Figure 1 so as to match in each case the experimental cross section for the 0^+ transition at the maximum near 30°. For the CCBA calculations the resulting value of D_0^2 was 20×10^4 $MeV^2 fm^3$, which is close to the usual value[10] required in (p,t) reactions, and for the DWBA calculations it was 63×10^4 MeV^2 fm^3. Thus, the strength for the ground-to-ground transition is increased by more than a factor of 3 by the inclusion of the inelastic coupling. As has been observed previously,[11]

there are two important ways in which transfer-reaction calculations using a coupled-channel description of the projectile-target relative motion differ from those using a simple one-channel distorted wave description. The obvious difference is the addition of effects from transfer routes other than those which directly connect the initial and final state, that is, the introduction of multistep processes. But in addition, the de-excitation processes introduced in a coupled-channel description of inelastic scattering alter the incoming and outgoing distorted waves from what they would be in a simple one-channel description, an effect which can be looked upon as an explicit renormalization of the one-channel optical potential. When the cross sections for inelastic scattering are large, as they are for highly collective nuclei, the de-excitation processes can produce a significant change in the strength of even the strongest transitions in transfer reactions.[11,12] (Of course, it is possible to simulate this effect to a certain extent by readjusting the parameters of the optical-model potential used in the DWBA calculation.) The importance of the de-excitation processes can be determined by including in a CCBA calculation only the transfer route from the initial to the final state, that is, by eliminating the multistep processes. We have performed such a calculation and have found that de-excitation effects account for most of the difference between the $^{22}Ne(p,t)$ ground-state cross sections calculated using the CCBA and those using the DWBA. It is interesting, however, that in this case the addition of the de-excitation processes increases the cross section whereas in other cases where this effect has been noted[11,12] most of which are at lower energies, the cross section is decreased.

In order to ascertain the significance of the discrepancies between the experimental cross sections and CCBA predictions, we investigated the sensitivity of the cross sections to reasonable variations of optical-model and deformation parameters. The deformation parameters used by Olsen et al. were based on analyses of 24.5 MeV proton inelastic scattering cross-sections and polarization data[13] on ^{20}Ne and ^{22}Ne, but with some arbitrary adjustments. The solid lines in Figure 2 show CCBA calculations, also using the deformation parameters determined in reference 13, but with the only adjustment being the standard requirement that the deformation lengths remain unchanged; that is, the β_λ were adjusted so as to keep $\delta_\lambda=\beta_\lambda R$ constant, where R is the optical model radius. This parameter set is listed as #2 in Table 2. Since deformation parameters determined from inelastic scattering at different energies and with different projectiles are not completely consistent, we also tried CCBA calculations using two other sets of deformation parameters. The parameter set labelled #3 in Table 2 is based on 104 MeV α-particle scattering,[14] again with adjustments to keep the deformation lengths constant. The set labelled #4 in Table 2 was determined by considering the deformation parameters to be merely parameterizations of inelastic scattering. In this case one should use ^{22}Ne deformation parameters based on proton scattering at the beam energy of the (p,t) reaction and ^{20}Ne deformation parameters from triton scattering at the outgoing triton energy of the (p,t) reaction. Accordingly, we determined a ^{22}Ne set by fitting 40 MeV proton scattering data.[15] We approximated the t + ^{20}Ne system by fitting 36 MeV ^{3}He scattering[16] on ^{20}Ne. CCBA calculations using these parameters are shown as the long- and short-dashed lines respectively in Figure 2.

The optical-model parameter set #1 of Table 1 was used in all the calculations shown in Figure 2.

In Figure 3 we show calculations using alternative sets of optical-model parameters. The solid curves show again calculations using parameter set #1. The long-dashed curves indicate the results of calculations using "average" parameters, based on fits by Becchetti and Greenlees to proton[17] and mass-3[18] scattering over a large range of target mass and projectile energy. This set is listed as #2 in Table 1. The calculations represented by the short-dashed curves were performed using a parameter set which has been found[19] to give good DWBA fits to (p,t) angular distributions for light nuclei. This set is labelled #3 in Table 1. The deformation parameters used for all the calculations shown in Figure 3 were those determined by de Swiniarski et al.[13] (listed as set #2 in Table 2). For each calculation shown in Figures 3 and 4 the strength constant D_o^2 was adjusted to reproduce the experimental 0^+ cross section at the maximum near 30°. The required values of D_o^2 deviated by as much as 50% from that used for the calculation shown in Figure 1.

A comparison of the curves in Figures 2 and 3 show that reasonable variations in optical-model and deformation parameters result in significant changes in the shapes of angular distributions. Thus, much of the difference between calculated and experimental angular distributions can be attributed to uncertainties in the optical-model and deformation parameters, although it may perhaps be significant that all calculations shown in the figures substantially underpredict the 2^+ cross section near 70°. On the other hand, the relative strengths of the cross sections are well predicted by the calculations and these are not much affected by parameter

variations. (Changes in the absolute magnitude of the cross sections are somewhat larger.) It should be added that other higher-order reaction mechanisms not included in the CCBA calculations may also contribute and could account for some of the remaining discrepancies. In view of all these uncertainties, we conclude that the ls-0d shell-model wavefunctions used with a CCBA reaction model are reasonably successful in predicting the cross section for ^{22}Ne(p,t) to the ground band of ^{20}Ne.

4. RESULTS: ^{24}Mg(p,t)^{22}Mg

The ^{24}Mg(p,t) reaction is a somewhat more interesting example than ^{22}Ne(p,t), since DWBA predictions for the transition to the first 2^+ state in ^{22}Mg underpredict the cross section by nearly two orders of magnitude. This is shown in Figure 4 where DWBA calculations are compared with the data of Paddock[20] and Nolen et al.,[21] taken at 42 MeV incident proton energy. This discrepancy is particularly surprising, since other known properties of the first T=1 2^+ state in the A=22 isobars (the static quadrupole moment, the B(E2) values for the transitions connecting it with the first 0^+ and first 4^+ states, and spectroscopic factors for single-nucleon transfer from A=21 and A=23 nuclei) seem to be in accord with the shell-model predictions. However, the shell-model wavefunctions also predict large strengths for two-nucleon transfer transitions connecting this state with excited states of ^{24}Mg. In particular, a very large transition from the first 2^+ state in ^{24}Mg is predicted. Similarly, transfer to the ground state of ^{22}Mg accompanied by inelastic excitation to the 2^+ is likely to be important. This is reminiscent of the situation for single-nucleon stripping and pickup reactions to $7/2^+$ and $9/2^+$

members of rotational bands of odd-A nuclei in this mass region, where direct transfer within a ls-0d shell space is forbidden but transfer accompanied by inelastic excitations is allowed. In these cases the measured cross sections appear to be understandable when multistep effects are included in the calculations.[22]

The solid curves in Figure 4 show the results of CCBA calculations using shell-model-based transfer amplitudes and allowing only a 0^+-2^+ inelastic coupling in the initial and final nuclei. This coupling space includes the two routes to the 2^+ state which are expected to be most important. The optical-model parameters used in the calculations shown in this figure are the same as those of reference 9 (set #1 in Table 1) and were chosen because of their relative success in reproducing the shapes of the angular distributions in ^{22}Ne(p,t). The deformation parameters used were taken from the analysis[13] of 24.5 MeV proton inelastic scattering on ^{22}Ne and ^{24}Mg. The deformation parameters are listed in Table 4 and the two-nucleon transfer amplitudes in Table 5. Multistep processes clearly have a dramatic effect on the 2^+ cross section. In fact, calculations within the 0^+-2^+ coupling space appear to overpredict the cross section.

If the first 0^+, 2^+, and 4^+ states are assumed to be members of an axially-symmetric rotational band in both ^{22}Mg and ^{24}Mg, a CCBA calculation using a 0^+-2^+-4^+ coupling space can be performed, simliar to those discussed in Section 3. The results of such a calculation using the same parameters as those used for the calculations of Figure 4 are shown in Figure 5. The data again are those of Paddock and Nolen et al. The value of D_o^2 has been adjusted to reproduce the strength of the 0^+ cross section at

its maximum near 30°. For the CCBA calculations, the value required was 32×10^4 MeV^2 fm^3 and for the DWBA calculations, 41×10^4 MeV^2 fm^3, both of which are rather large compared to the standard value. As in the ^{22}Ne(p,t) case, the difference between the ground-to-ground strength calculated using the CCBA and that calculated using the DWBA is largely the result of de-excitation effects.

A comparison between Figures 4 and 5 indicates that the coupling to the 4^+ states reduces the magnitude of the calculated 2^+ cross section and thus improves its agreement with the measured cross section. This is largely due to the strong transition between the 2^+ state of ^{24}Mg and the 4^+ state of ^{22}Mg accompanied by inelastic de-excitation to the 2^+ state. On the other hand, the slope of the 2^+ angular distribution is in disagreement with the data and the cross section for the 4^+ transition is badly over-predicted. We have also tried reasonable variations in the optical-model and deformation parameters, and as with the ^{22}Ne(p,t) case, these variations had some effect on the predicted shapes of the angular distributions but very little effect on the relative magnitudes. Thus, the remaining magnitudes discrepancies appear to be significant.

It is possible that these discrepancies represent deficiencies in the shell-model wavefunctions. However, it seems more likely that the problems arise from the probability that the 0^+-2^+-4^+ coupling space in ^{24}Mg is too small. A 2^+-3^+-4^+ level sequence lies at an energy just above that of the 4^+ level, and these states are known to possess strong inelastic coupling with the first 0^+, 2^+, and 4^+ states.[23] In addition, shell-model predictions for transitions from these states to the ^{22}Mg states are large in some cases. For example, the transitions from the second 2^+ state of

^{24}Mg to the 2^+ and 4^+ states of ^{22}Mg and from the second 4^+ state of ^{24}Mg to the 4^+ state of ^{22}Mg are predicted to be strong. It is quite possible that the inclusion of these transitions in the calculation might improve not only the magnitude of the 4^+ cross section but also the shape of the 2^+ angular distribution. In principle one could perform a CCBA calculation including these states in the coupling space, assuming they form a band based on a very strong γ-vibration or alternatively that they constitute the extension of the ground band of a rigid triaxial rotor. However, this results in a calculation with a large space and involving considerable uncertainties in the description of the inelastic couplings. We have not yet attempted such a calculation.

Another souce of uncertainty in both the ^{24}Mg(p,t) and the ^{22}Ne(p,t) calculations concerns our use of the collective model to generate the inelastic form factors. It is questionable whether this model is completely adequate to describe inelastic excitations of nuclei containing as few nucleons as those considered here. Of course, we guarantee that this description is approximately correct by adjusting the parameters of the model to fit inelastic scattering. However, detailed differences between the collective-model form factors and the physical form factors could significantly affect the results of CCBA calculations, particularly when many routes of similar strength are contributing to a single transition as is the case for the 2^+ transition in ^{24}Mg(p,t). It would therefore be interesting to compare the results presented here with CCBA calculations using inelastic form factors based on shell-model wavefunctions. Some indication of the differences one might observe can be obtained by comparing the inelastic form

factors. Except for the strengths, which must be renormalized in the shell-model case to account for core-polarization effects,[1] the quadrupole (L=2) form factors are qualitatively similar in the two models. However, in the A=22 and A=24 cases, the shell-model wavefunctions yield nodeless hexadecapole (L=4) inelastic form factors, but the collective model predicts a node near the nuclear surface. The reason for this is clear when one notes that β_4 is small in these two systems and thus the collective-model inelastic form factors for L=4 is dominated by the second-derivative term in the expansion of the nuclear surface (Equation 6.11 of reference 8). In A=20, where β_4 is large, the first derivative term is dominant and the collective-model L=4 form factors are nodeless, in agreement with shell-model predictions. Since, as has been mentioned, the effect on the ^{22}Ne(p,t) calculations of including the 4^+ state of ^{22}Ne is small, the use of shell-model inelastic form factors is unlikely to significantly change the results. However, in the ^{24}Mg(p,t) case, the effects should be more important and use of the shell-model form factors may provide a better fit to the data.

5. SUMMARY AND CONCLUSIONS

In this paper we have studied the comparison between measured cross sections for ^{22}Ne(p,t)^{20}Ne and ^{24}Mg(p,t)^{22}Mg and predictions of shell-model wavefunctions within the framework of a coupled-channel Born approximation reaction analysis. We have seen that the effects of the multistep reaction processes are significant, in the ^{22}Ne(p,t) case causing mainly changes in the angular distribution shapes but for ^{24}Mg(p,t) leading to large magnitude changes as well. Thus, it is essential to include multistep effects

in the reaction analysis in order to make a meaningful test of microscopic wavefunctions.

We have explored the effect of uncertainties in the parameters involved in the CCBA calculations. We found that reasonable variations in such parameters lead to non-negligible changes in the predicted shapes of some angular distributions but have little effect on the predictions for the relative magnitudes of the transitions. With these uncertainties taken into account, the agreement between shell-model predictions and measured cross sections for the ^{22}Ne(p,t) reaction to the ground-state rotational band in ^{20}Ne appears to be reasonably good. For the ^{24}Mg(p,t) reaction, on the other hand, although the CCBA calculations show that much of the apparent discrepancy in the prediction of the cross section for the transition to the first 2^+ state can be understood as the effect of multistep processes, significant discrepancies remain, such as the overprediction of the 4^+ cross section by a factor of 10. We feel, however, that these discrepancies are less likely to be due to inadequacies in the shell-model wavefunctions than to a coupling space in the reaction calculation which was too restrictive. In particular, transitions from the second 2^+ and 4^+ states of ^{24}Mg, which were ignored in these calculations, are calculated to be strong from shell-model wavefunctions.

There are other uncertainties in our reaction model which make it difficult to draw firm conclusions about the quality of shell-model wavefunctions from calculations such as these. One cannot rule out, for example, the possible importance of higher-order reaction processes not included in the CCBA model, such as the successive transfer mechanism (e.g., (p,d) + (d,t)). Also, the

collective-model yields inelastic form factors which are only approximately valid, and this may be the cause of some of the discrepancies between the calculations and experimental data. Thus, although the ^{22}Ne(p,t) results are relatively good and it is possible to understand qualitatively the discrepancies of the ^{24}Mg(p,t) case in terms of an inadequate calculation space, further calculations which include some of these additional effects would be useful.

The authors would like to acknowledge many valuable discussions with R.J. Ascuitto and H. Nann during the course of this work.

REFERENCES

1. W.G. Love and G.R. Satchler, Nucl. Phys. A101 (1967) 424.
2. S.K. Penney and G.R. Satchler, Nucl. Phys. 53 (1964)145; T. Tamura, Ann. Rev. Nucl. Sci. 19 (1969)99.
3. R.J. Ascuitto and N.K. Glendenning, Phys. Rev. 181 (1969)1396.
4. R.J. Ascuitto, unpublished.
5. W. Chung and B.H. Wildenthal, to be published.
6. P.D. Kunz, unpublished.
7. B.F. Bayman and A. Kallio, Phys. Rev. 156 (1967)1121.
8. N.K. Glendenning, Proc. Int. School of Physics "Enrico Fermi", course XL (1967), ed. M. Jean and R.A. Ricci (Academic Press, New York, 1969) p.332.
9. D.K. Olsen, T. Udagawa, T. Tamura, and R.E. Brown, Phys. Rev. C8 (1973)609.
10. H.W. Baer, J.J. Kraushaar, C.E. Moss, N.S.P. King, R.E.L. Green, P.D. Kunz, and E. Rost, Ann. Phys. (N.Y.) 76 (1973)437.
11. R.J. Ascuitto, C.H. King, L.J. McVay, and B. Sørensen, Nucl. Phys. A226 (1974)454.
12. R.J. Ascuitto, N.K. Glendenning, and B. Sørensen, Nucl. Phys. A183 (1972)60.
13. R. de Swiniarski, C. Glashausser, D.L. Hendrie, J. Sherman, A.D. Bacher, and E.A. McClatchie, Phys. Rev. Lett. 23 (1969) 317; R. de Swiniarski, A.D. Bacher, F.G. Resmini, G.R. Plattner, D.L. Hendrie, and J. Raynal, Phys. Rev. Lett 28 (1972)1139.
14. H. Rebel, G.W. Schweimer, G. Schatz, J. Specht, R. Löhken, G. Hauser, D. Habs, and H. Klewe-Nebenius, Nucl. Phys. A182 (1972)145.
15. D.G. Madland, Ph.D. Thesis, Univ. of Minnesota (1970), unpublished.

16. K.P. Artemov, V.Z. Goldberg, and V.P. Rudakov, Yadern. Fiz. 9 (1969)266, 1173 (translation: Sov. J. Nucl. Phys. 9 (1969) 157, 686).

17. F.D. Becchetti, Jr., and G.W. Greenlees, Phys. Rev. 182 (1969)1190.

18. F.D. Becchetti, Jr. and G.W. Greenlees, in Polarization phenomena in nuclear reactions, ed. H.H. Barschall and W. Haeberli (University of Wisconsin Press, Madison, 1970) p. 682.

19. H. Nann, W. Benenson, W.A. Lanford, and B.H. Wildenthal, Phys. Rev. C10 (1974)1001.

20. R.A. Paddock, Phys. Rev. C5 (1972)485.

21. J.A. Nolen, Jr., W. Benenson, D. Larson, I.D. Proctor, and B.H. Wildenthal, Contributions to the symposium on two-nucleon transfer and pairing excitations (Argonne, Ill., Mar. 20, 1972) unpublished.

22. H. Schulz, H.J. Wiebicke, R. Fülle, D. Netzband, and K. Schlott, Nucl. Phys. A159 (1970)324; R.S. Mackintosh, Nucl. Phys. A170 (1971)353; A.K. Abdallah, T. Udagawa, and T. Tamura, Phys. Rev. C8 (1973)1855; and R.O. Nelson and N.R. Roberson, Phys. Rev. C6 (1972)2153.

23. A.A. Rush and N.K. Ganguly, Nucl. Phys. A117 (1968)101.

24. J.B. French, E.C. Halbert, J.B. McGrory, and S.S.M. Wong, Advances in nuclear physics, ed. M. Baranger and E. Vogt, vol. 3 (Plenum, New York, 1969) p. 193.

FIGURE CAPTIONS

Figure 1--Comparison of CCBA (solid lines) and DWBA (dashed lines) calculations with the data of Olsen et al.[9] for the differential cross sections of ^{22}Ne(p,t) at 39.8 MeV to the 0^+(g.s.), 2^+ (1.63 MeV), and 4^+ (4.25 MeV) states of ^{20}Ne. The optical-model parameters used in the calculations are listed as set #1 in Table 1, the deformation parameters are listed as set #1 in Table 2, and the spectroscopic amplitudes are listed in Table 3.

Figure 2--The data of Olsen et al.[9] for ^{22}Ne(p,t) are compared with three CCBA calculations using the same optical-model parameters (set #1 of Table 1) but different deformation parameters. The calculations shown as solid lines used parameter set #2 of Table 2, those shown as long dashed lines used parameter set #3, and those shown as short dashed lines used parameter set #4. The calculations using parameter sets #3 and #4 gave essentially identical results for the ground-state cross section.

Figure 3--The data of Olsen et al.[9] for ^{22}Ne(p,t) are compared with three CCBA calculations using the same deformation parameters (set #2 of Table 2) but different optical-model parameters. The calculations shown as solid lines used parameter set #1 of Table 1. Those shown as long-dashed lines used parameter set #2, and those shown as short-dashed lines used parameter set #3.

Figure 4--Comparison of CCBA (solid lines) and DWBA (dashed lines) calculations with the data of Paddock[20] and Nolen et al.[21] for the differential cross sections of ^{24}Mg(p,t) at 42.0

MeV to the 0^+ (g.s.) and 2^+ (1.25 MeV) states of ^{22}Mg. The optical-model parameters used in the calculations were those listed as set #1 of Table 1, the deformation parameters are listed in Table 4, and the spectroscopic amplitudes are listed in Table 5. The CCBA calculation utilized a 0^+-2^+ coupling space.

Figure 5--The same cross sections are shown as in Figure 4 plus that of the transition to the 4^+ (3.31 MeV) state. Again the dashed lines represent DWBA calculations. The solid lines indicate the results of CCBA calculations using the same optical-model and deformation parameters as the calculations shown in Figure 4 but with a 0^+-2^+-4^+ coupling space.

Table 1--Optical-model parameters.

Parameter Set	Channel	V_R	R_R	a_R	W_V	W_{SF}	r_I	a_I	r_C	Ref.
1	p+^{22}Ne	55.2	1.11	0.57	6.2	8.2	1.11	0.50	1.11	9
	t+^{20}Ne	160.4	1.20	0.72	25.0	0.0	1.40	0.84	1.30	9
2	p+^{22}Ne	44.8	1.17	0.75	6.1	2.9	1.32	0.57	1.09	17
	t+^{20}Ne	159.3	1.20	0.72	34.8	0.0	1.40	0.84	1.30	18
3	p+^{22}Ne	45.5	1.20	0.70	0.0	13.0	1.25	0.70	1.25	19
	t+^{20}Ne	173.9	1.15	0.72	20.6	0.0	1.50	0.82	1.40	19

Definition of parameters: ref. 17.

Table 3--Spectroscopic amplitudes[a] for ^{22}Ne(p,t).

J^π (^{22}Ne)	J^π (^{20}Ne)	J[b]	$d^2_{5/2}$	$s^2_{1/2}$	$d^2_{3/2}$	$d_{5/2}s_{1/2}$[c]	$d_{5/2}d_{3/2}$	$s_{1/2}d_{3/2}$
0^+	0^+	0	-0.8180	-0.2341	-0.2853			
	2^+	2	-0.2251		-0.0332	-0.1826	0.2810	-0.0588
	4^+	4	0.8410				0.3474	
2^+	0^+	2	0.2485		0.0438	0.1325	0.1790	0.0782
	2^+	0	-0.6533	-0.1262	-0.2297			
		2	-0.1304		0.0005	0.0791	-0.1644	-0.0161
		4	0.5876				0.1941	
	4^+	2	-0.3392		-0.0645	-0.2716	0.1598	-0.0974
		4	-0.4920				-0.2065	
4^+	0^+	4	0.3800				0.0515	
	2^+	2	0.4198		0.0768	0.2144	0.1697	0.1063
		4	-0.3212				-0.1167	
	4^+	0	-0.4514	-0.0133	-0.1498			
		2	-0.1355		0.0099	0.1645	-0.1474	0.0150
		4	0.4722				0.1598	

a) Calculated from the shell-model wavefunctions of ref. 5. The definition used for these amplitudes is that of ref. 24.

b) Total transferred angular momentum.

c) For those amplitudes which involve two different single-particle orbitals, the order of the orbitals as listed at the top of the column indicates the order of coupling to J.

Table 2.--Deformation lengths[a] used in ^{22}Ne(p,t) calculations.

Parameter Set	Nucleus	δ_2	δ_4	Reference
1	^{22}Ne	1.40	0.156	9
	^{20}Ne	1.466	0.814	9
2	^{22}Ne	1.384	0.146	13
	^{20}Ne	1.290	0.769	13
3	^{22}Ne	1.253	0.072	14
	^{20}Ne	1.303	0.410	14
4	^{22}Ne	1.555	0.233	-
	^{20}Ne	1.303	0.410	-

a) The deformation lengths are related to the deformation parameters β_λ via $\delta_\lambda = \beta_\lambda r_R A^{1/3}$, where $r_R A^{1/3}$ is the real optical-model radius.

Table 5.-- Spectroscopic amplitudes[a] for ^{24}Mg(p,t).

$J^\pi(^{24}Mg)$	$J^\pi(^{22}Mg)$	J	$d^2_{5/2}$	$s^2_{1/2}$	$d^2_{3/2}$	$d_{5/2}s_{1/2}$	$d_{5/2}d_{3/2}$	$s_{1/2}d_{3/2}$
0^+	0^+	0	-1.2354	-0.3860	-0.5573			
	2^+	2	-0.1274		0.0736	-0.1237	0.5550	0.0767
	4^+	4	1.5970				0.6724	
2^+	0^+	2	0.3737		0.1331	0.2688	0.3014	0.2189
	2^+	0	-1.0712	-0.2495	-0.4913			
		2	-0.2456		-0.0555	0.0228	-0.2689	-0.1356
		4	0.8150				0.2903	
	4^+	2	-0.5297		-0.0547	-0.4543	0.3356	-0.1450
		4	-0.8377				-0.3856	
4^+	0^+	4	0.4399				0.0887	
	2^+	2	0.6403		0.2179	0.4331	0.3322	0.3250
		4	-0.4708				-0.1921	
	4^+	0	-0.6968	0.0145	-0.3291			
		2	-0.3300		0.0039	0.3200	-0.1601	-0.0611
		4	0.6638				0.2994	

a) Calculated from the shell-model wavefunctions of ref. 5. See Table 3 for definitions.

Table 4.-- Deformation lengths[a] used in ^{24}Mg(p,t) calculations.

Nucleus	δ_2	δ_4	Reference
^{24}Mg	1.655	-0.176	13
^{22}Mg	1.382	0.148	13

a) See Table 2 for definitions.

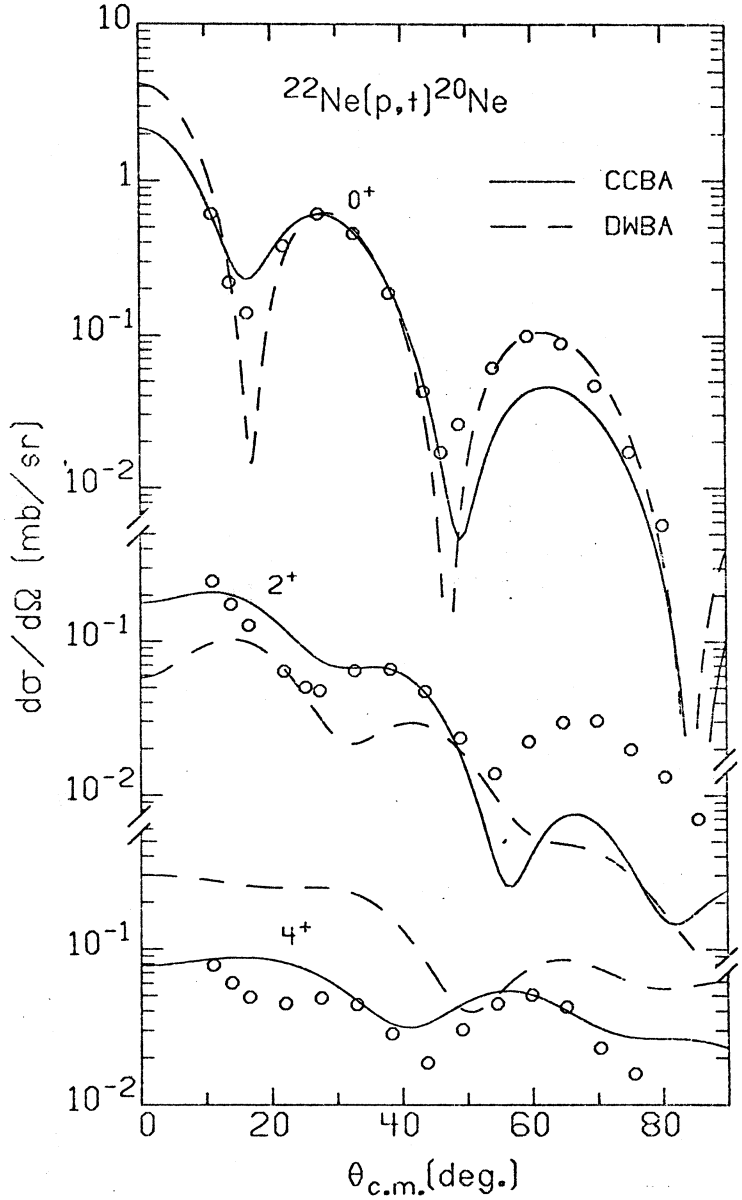
^{22}Ne(p,t)^{20}Ne
CCBA
DWBA
0$^+$
2$^+$
4$^+$
dσ/dΩ (mb/sr)
θ$_{c.m.}$(deg.)

Fig. 1

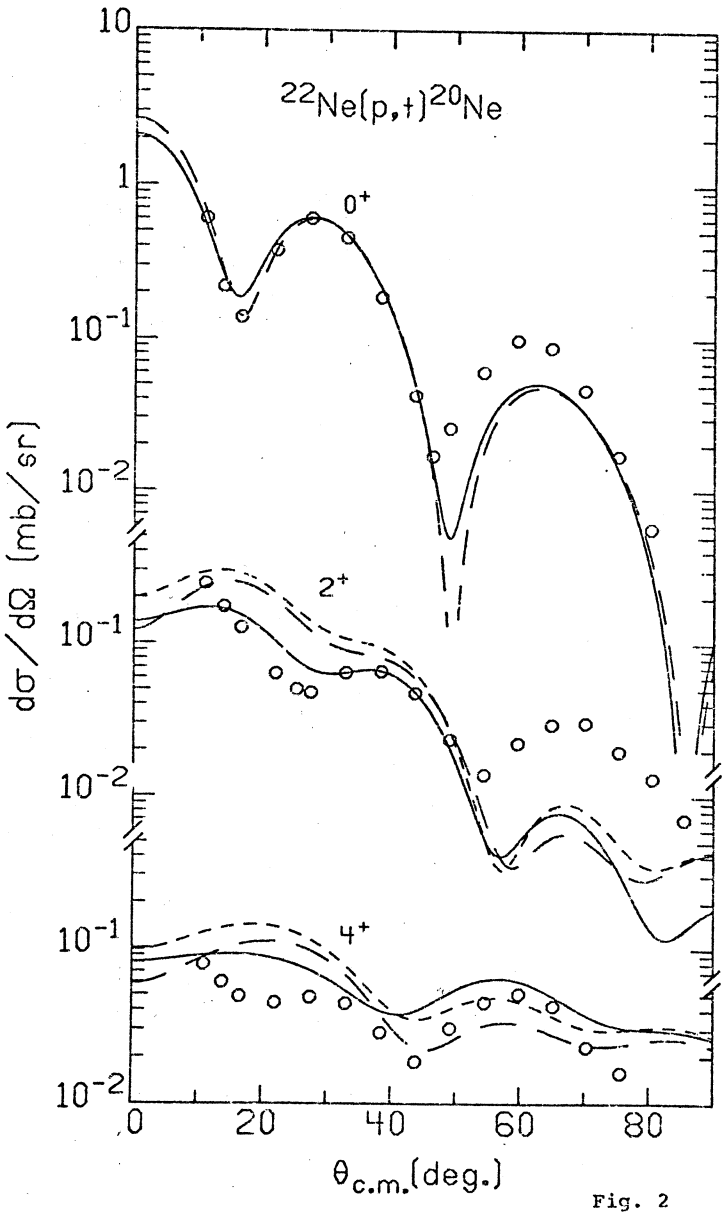
^{22}Ne(p,t)^{20}Ne
0$^+$
2$^+$
4$^+$
dσ/dΩ (mb/sr)
θ$_{c.m.}$(deg.)

Fig. 2

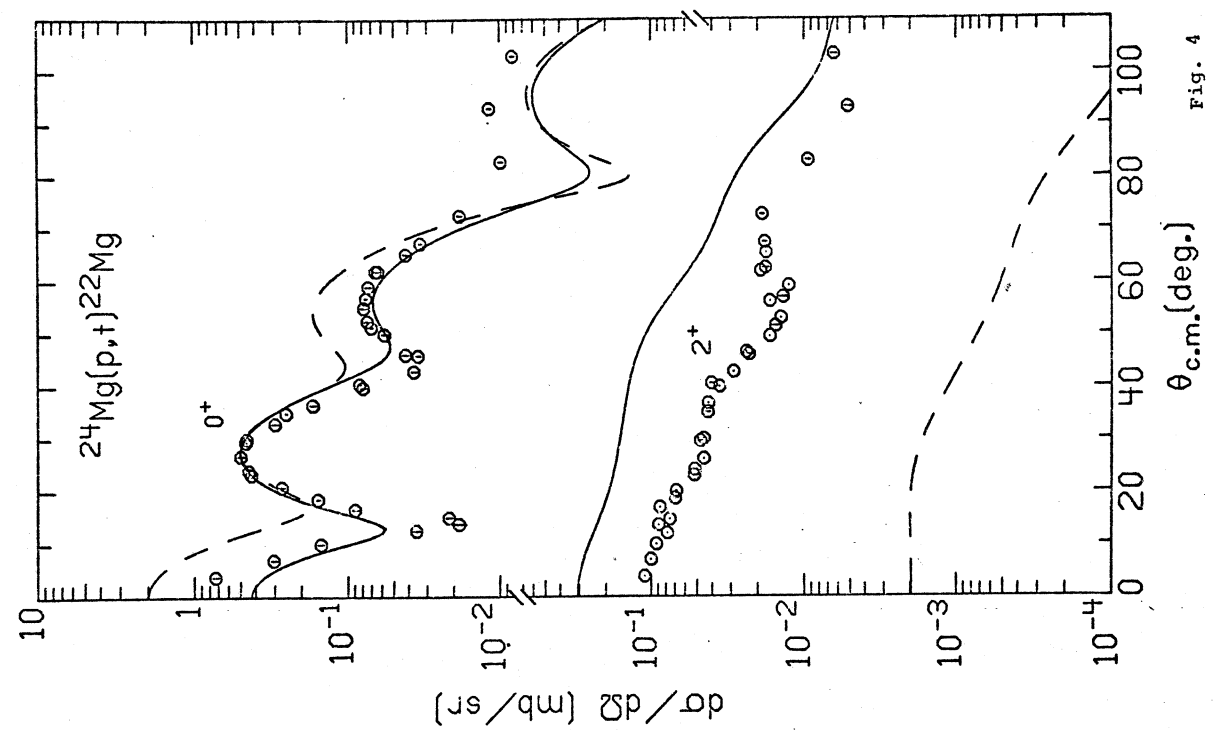
^{24}Mg(p,t)^{22}Mg
0$^+$
2$^+$
dσ/dΩ (mb/sr)
θc.m.(deg.)

Fig. 4

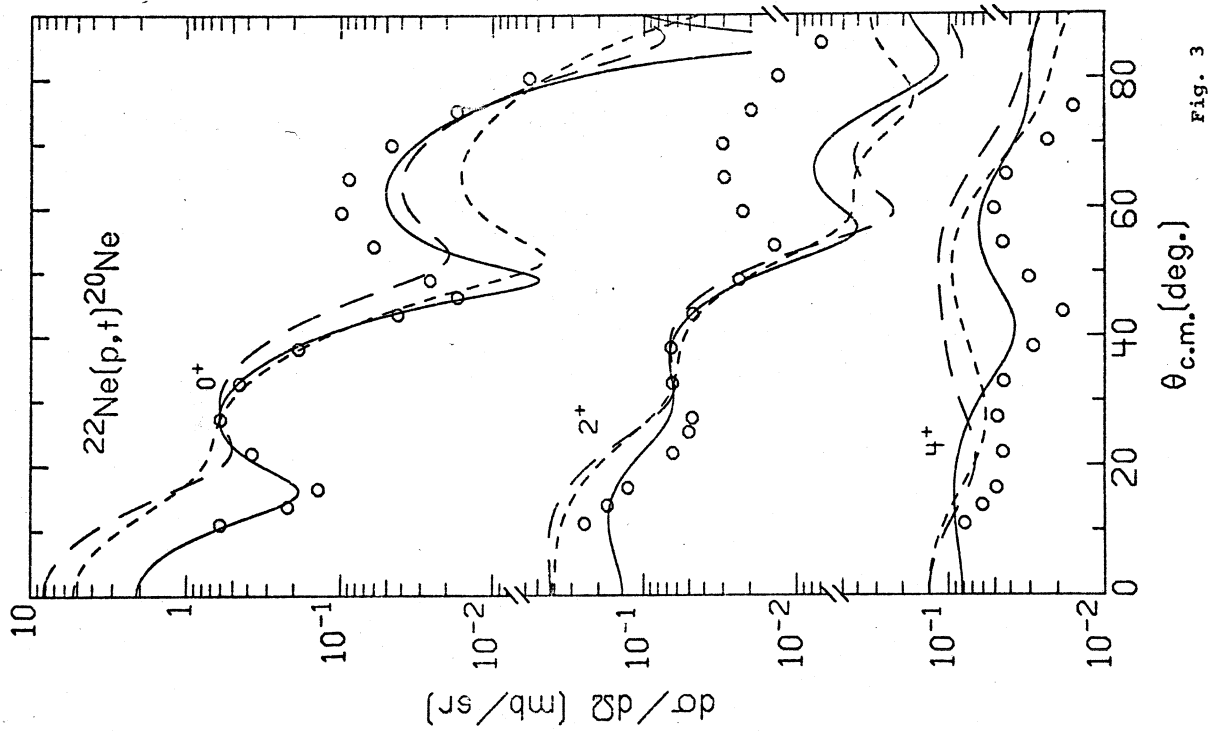
^{22}Ne(p,t)^{20}Ne
0$^+$
2$^+$
4$^+$
dσ/dΩ (mb/sr)
θc.m.(deg.)

Fig. 3

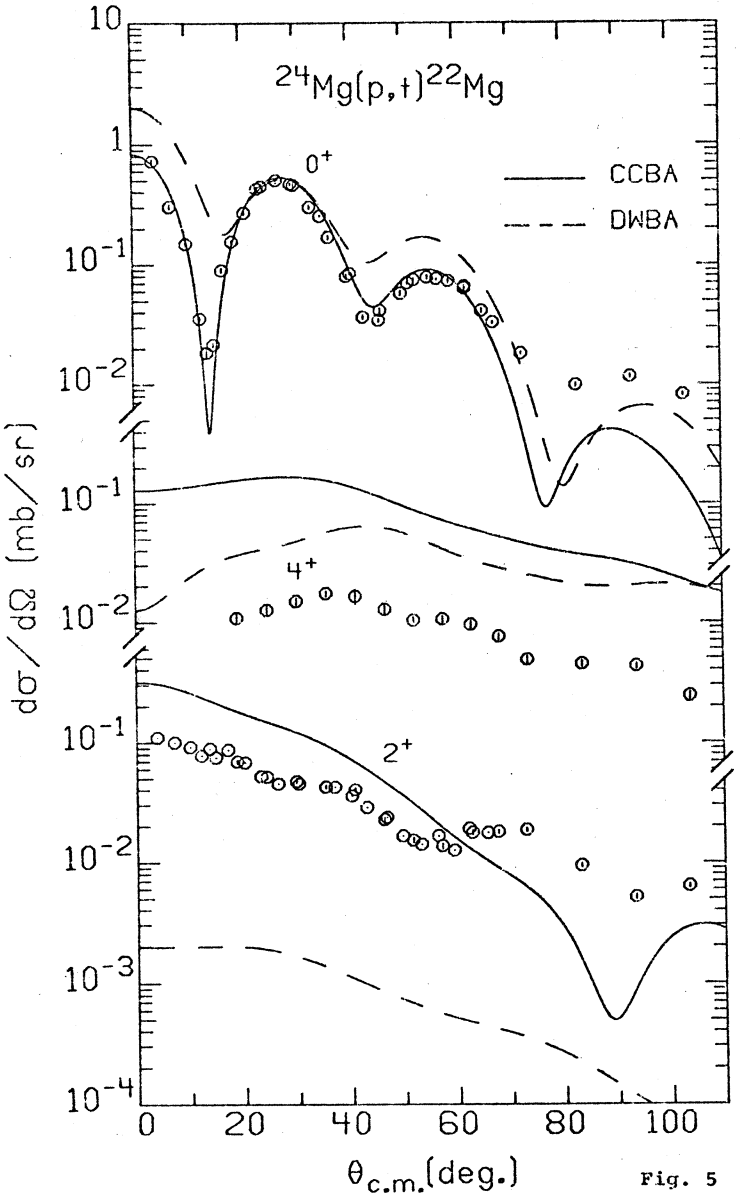
$^{24}Mg(p,t)^{22}Mg$
0^+
4^+
2^+
CCBA
DWBA
$d\sigma/d\Omega$ (mb/sr)
$\theta_{c.m.}$(deg.)
10
1
10^{-1}
10^{-2}
10^{-3}
10^{-4}
0
20
40
60
80
100

Fig. 5